

Algorithms for Voltage Control in Distribution Networks

Guido Cavraro
University of Padova
Padova, Italy
Email: cavraro@dei.unipd.it

Ruggero Carli
University of Padova
Padova, Italy
Email: carlirug@dei.unipd.it

Abstract—We consider the problem of exploiting the micro-generators connected to the power distribution grid to provide distributed reactive power compensation for voltage support. We review some of the state-of-the-art control strategies, compare and analyze their performance. Furthermore, we propose a novel control strategy that, exploiting communications among neighboring micro-generators, achieves a fast voltage regulation and minimizes the losses of the grid. Simulations are provided in order to confirm the effectiveness of the novel algorithm and to compare its performance with respect to the performance of the state-of-the-art algorithms. In addition, a discussion on the fundamental role played by the communication among generators to guarantee that voltage constraints are satisfied is included.

I. INTRODUCTION

The advent of distributed energy resources such as wind turbines, solar cells, or other renewable energy sources is dramatically changing the actual power distribution scenario [1]. In fact, a massive number of small power generators are envisioned to be deployed in the low and medium voltage power distribution grid. The integration of the distributed energy resources in the distribution network could yield to a number of benefits for the electrical distribution system, e.g. voltage profile improvements, reduction of line losses, reduction of power generation cost and other ancillary services [2]. On the other hand, an uncontrolled power injection of several renewable energy sources could lead to system instabilities or damages, if not properly regulated. In fact, the intermittence of the renewable sources can cause large voltages variations and operational bounds may be violated. For these reasons, voltage regulation is a fundamental issue in the development of the future *smart distribution grid*.

Voltage regulation is achieved by controlling the generators reactive power output, mainly because reactive power can be produced almost with no cost and does not withstand to economical issue, as instead the active power does. Traditionally, the voltage control is performed using mechanical control devices, such as shunt capacitor banks or on-load tap changers [3], that often are too slow to respond properly to the voltage fluctuation due to the variability of the energy resources and of the load demand. These are the reasons that lead to the recent interest for strategies that regulate the voltage magnitudes in the distribution network by acting the injection (or absorption) of the micro-generators reactive power. Many inverters have the capability, when they are running below their rated output current, to inject (or to absorb) reactive power together with active power [4]. Inverters can act in the grid on a fast timescale. Furthermore generators can connect or disconnect, requiring an automatic reconfiguration of the grid control infrastructure (the so called “plug and play” approach).

These reasons call for local or distributed approaches to face with the voltage regulation problem. Among the purely local strategies, we cite the conservation of fixed power factor, the injection of constant reactive power, the reactive power control dependent on the voltage, and the power factor control dependent on the active power injection (see [5], [6], [7], [8]). These strategies however aim to only guarantee that the voltage constraints are satisfied. Other strategies instead take into account other important objectives, like loss minimization, approaching the system state towards *optimal* configurations, solutions of the *optimal reactive power flow* (OPRF) problem. In the traditional transmission grid the OPRF problem is typically solved by centralized solvers that collect all the necessary field data, compute the optimal configuration, and dispatch the power production to the generators. However this approach is not practical in the distribution network, because of the fast variability in the power demand and in the generators’ generation capabilities. Recently, popular solutions reformulate the ORPF problem as a rank-constrained semidefinite program, convexify it by dropping the rank constraint and then solve it in a distributed way (see [9], [10], [11]). This approach however requires that all the buses of the grid are monitored, which is not practical in the distribution network. Instead, the algorithms proposed in [12] and [13] are scalable in the number of generators and do not require monitoring of all the buses of the grid. They consist of the iteration of the two following actions: collecting voltage measurements at the micro-generators buses and actuating control laws based on these measured data. In this paper we first revise three of the state-of-the-art voltage control algorithms. Two of them are purely local, i.e. agents execute them just by using measurements of their own voltages, without cooperation. They have a fast convergence to the steady state, even if it is not guaranteed that voltage constraints are satisfied. On the other hand, the third strategy allows the agents to cooperate with each other and achieves power loss minimization while guaranteeing that voltages constraints are satisfied. However this strategy exhibits a transient which is slower as compared to the other two strategies. In the second part of the paper we propose a novel algorithm that combines the good properties of the previous strategies: fast transient, voltage constraints are satisfied and power loss minimization. The rest of the paper is organized as follows. In Section III we provide a model for the distribution network. In Section IV, we revise the state-of-the-art control strategies. In Section V, we propose the novel control strategy and finally, we analyze and compare the strategies performance in Section VI.

II. MATHEMATICAL PRELIMINARIES AND NOTATION

Let $\mathcal{G} = (\mathcal{V}, \mathcal{E}, \sigma, \tau)$ be a directed graph, where \mathcal{V} is the set of nodes, \mathcal{E} is the set of edges, with $n = |\mathcal{V}|$, $r = |\mathcal{E}|$. Moreover $\sigma, \tau : \mathcal{E} \rightarrow \mathcal{V}$ are two functions such that edge $e \in \mathcal{E}$ goes from the source node $\sigma(e)$ to the terminal node $\tau(e)$. A *path* is a sequence of consecutive distinct edges. Given a vector u , we denote by \bar{u} its (element-wise) complex conjugate, and by u^T its transpose. Let $A \in \{0, \pm 1\}^{r \times n}$ be the incidence matrix of the graph \mathcal{G} , defined via its elements

$$[A]_{ev} = \begin{cases} -1 & \text{if } v = \sigma(e) \\ 1 & \text{if } v = \tau(e) \\ 0 & \text{otherwise.} \end{cases}$$

We define by $\mathbf{1}$ the column vector of all ones, while by e_v we the vector whose value is 1 in position v , and 0 everywhere else. Given $u, v, w \in \mathbb{R}^\ell$, with $v_h \leq w_h, h = 1, \dots, \ell$ we define the operator $[u]_v^w$ as the component wise projection of u in the set $\{x \in \mathbb{R}^\ell : v_h \leq x_h \leq w_h, h = 1, \dots, \ell\}$, that is,

$$([u]_v^w)_h = \begin{cases} u_h & \text{if } v_h \leq u_h \leq w_h \\ v_h & \text{if } u_h < v_h \\ w_h & \text{if } u_h > w_h \end{cases} \quad (1)$$

III. CYBER-PHYSICAL MODEL OF A SMART POWER DISTRIBUTION GRID

In this work, we envision a *smart* power distribution network as a cyber-physical system, in which the *physical layer* consists of the power distribution infrastructure, including power lines, loads, microgenerators, and the point of connection to the transmission grid (called PCC), while the *cyber layer* consists of intelligent agents, dispersed in the grid. We model the physical layer as a directed graph \mathcal{G} , in which edges in \mathcal{E} represent the power lines, and nodes in \mathcal{V} represent both loads and generators that are connected to the microgrid (see Figure 1, middle panel). These include the residential and industrial consumers, microgenerators, and also the PCC. We limit our study to the steady state behavior of the system, where all voltages and currents are sinusoidal signals at the same frequency ω_0 , and can therefore be represented by phasors. The system state is described by the following variables (see Figure 1, lower panel):

- $u \in \mathbb{C}^n$, where u_v is the grid voltage at node v ;
- $i \in \mathbb{C}^n$, where i_v is the current injected at node v ;
- $s = p + iq \in \mathbb{C}^r$, where s_v, p_v and q_v are the complex, the active and the reactive power injected at node v .

For every edge e of the graph, we define by z_e the impedance of the corresponding power line. We make the following assumption.

Assumption 1: All power lines in the grid have the same inductance/resistance ratio, i.e., $z_e = e^{i\theta}|z_e|$, for any $e \in \mathcal{E}$ and for a fixed θ .

Assumption 1 is satisfied when the grid is relatively homogeneous, and is reasonable in most practical cases. We collect all the grid impedances absolute values in the matrix $Z = \text{diag}(|z_e|, e \in \mathcal{E})$. We label the PCC as node 1 and consider it as an ideal sinusoidal voltage generator (*slack bus*) at the grid nominal voltage U_N , with arbitrary, but fixed, angle ϕ . From now on, we consider, without loss of generality, $\phi = 0$. We model all nodes except the PCC as *constant power* or *P-Q buses*. The powers s_v corresponding to grid loads are

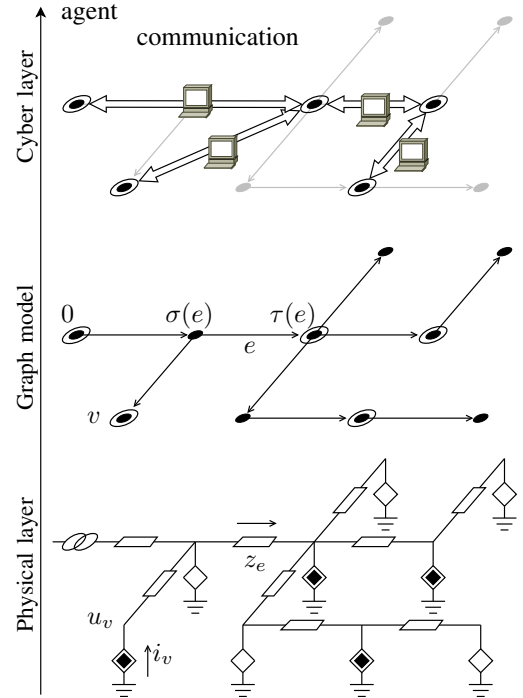


Figure 1. Schematic representation of a microgrid. In the lower panel the physical layer is represented via a circuit representation, where black diamonds are microgenerators, white diamonds are loads, and the left-most element of the circuit represents the PCC. The middle panel illustrates the corresponding graph representation. The upper panel represents the cyber layer, where agents (i.e. microgenerators and the PCC) are connected via a communication infrastructure.

such that $p_v < 0$, meaning that active power is *supplied* to the devices. On the other hand, the complex powers corresponding to micro-generators are such that $p_v \geq 0$, as active power is *injected* into the grid. The system state satisfies the equations

$$i = e^{-i\theta} Y u \quad (2)$$

$$u_1 = U_N \quad (3)$$

$$u_v \bar{i}_v = p_v + iq_v \quad v \neq 0 \quad (4)$$

where $e^{-i\theta} Y$ is the bus admittance matrix of the grid. It can be shown that there exists a unique symmetric, positive semidefinite matrix $X \in \mathbb{R}^{n \times n}$ such that

$$\begin{cases} XY = I - \mathbf{1}e_1^T \\ X e_1 = 0. \end{cases} \quad (5)$$

called the Green matrix, which depends only on the topology of the grid power lines and on their impedances, and whose elements are all not negative. Thanks to the Green matrix, we can express the voltages as a function of the currents via

$$u = e^{i\theta} X i + \mathbf{1}U_N. \quad (6)$$

We assume that every micro-generator corresponds to an *agent*, or *compensator*, in the cyber layer (upper panel of Figure 1), and belongs to the set $\mathcal{C} \subseteq \mathcal{G}$ (with $|\mathcal{C}| = m$). We assume furthermore that the agents are provided with some

- *sensing capabilities*, in particular *voltage phasor measurement unit* (PMU), a device that allows them to take phasorial measurements of the voltages ([14]);
- *computational capabilities* that will be exploited to implement the proposed algorithms.

The agents can command the amount of reactive power injected in the grid. In order to underline the difference among smart agents and passive loads, we introduce the following block decomposition of the voltages vector u

$$u = [u_1 \quad u_G^T \quad u_L^T], \quad (7)$$

where u_1 is the voltage at the PCC, $u_G \in \mathbb{C}^m$ are the voltages at the microgenerators, and $u_L \in \mathbb{C}^{n-m-1}$ are the voltages at the loads. Similarly, we also define $s_G = p_G + iq_G$ and $s_L = p_L + iq_L$. The non-linear relation among voltages and powers, can be explicitly approximate by the following proposition, which has been used in [13].

Proposition 2: Consider the physical model described by the system of nonlinear equations (6), (3) and (4). Compensators and load voltages satisfy

$$\begin{bmatrix} u_G \\ u_L \end{bmatrix} = \frac{e^{i\theta}}{U_N} \begin{bmatrix} M & N \\ N^T & Q \end{bmatrix} \begin{bmatrix} \bar{s}_G \\ \bar{s}_L \end{bmatrix} + \mathbf{1}U_N + o\left(\frac{1}{U_N}\right) \quad (8)$$

where the little-o notation means that $\lim_{U_N \rightarrow \infty} \frac{o(f(U_N))}{f(U_N)} = 0$.

The quality of this approximation relies on having large nominal voltage U_N and relatively small currents injected by the inverters (or supplied to the loads). This assumption is verified in practice, and corresponds to correct design and operation of power distribution networks, where indeed the nominal voltage is chosen sufficiently large (subject to other functional constraints) in order to deliver electric power to the loads with relatively small power losses on the power lines. Furthermore, (8) can be used to compute an approximation of the voltages magnitudes

$$\begin{bmatrix} |u_G| \\ |u_L| \end{bmatrix} = \frac{1}{U_N} \begin{bmatrix} M & N \\ N^T & Q \end{bmatrix} \begin{bmatrix} \cos(\theta)p_G + \sin(\theta)q_G \\ \cos(\theta)p_L + \sin(\theta)q_L \end{bmatrix} + \mathbf{1}U_N. \quad (9)$$

Equation (9) models the well known fact that the injection or the absorption of reactive power increase or decrease, respectively, the voltage magnitude also in the case of not purely inductive lines.

IV. VOLT/VAR CONTROL STRATEGIES

Classically, the amount of reactive power injected by the generators into the grid is regulated in order to perform the voltage control, namely, to maintain the bus voltage magnitudes within a predefined percentage deviation from the reference voltage U_N . In our setup, since we assume that only agents can measure their voltage, we consider the following set of constraints

$$U_{min} \leq |u_h| \leq U_{max}, \quad \forall h \in \mathcal{C} \quad (10)$$

where U_{min} and U_{max} are, respectively, the minimum and maximum admissible values for the voltage magnitudes. In addition to (10), since the generators deployed in the distribution network are, typically, of small size, we need to take into account also constraints on the generation capabilities of agent h . Precisely, we assume that

$$q_{min,h} \leq q_h \leq q_{max,h}, \quad \forall h \in \mathcal{C} \quad (11)$$

where $q_{min,h}$, $q_h \leq q_{max,h}$ denote, respectively, the minimum and the maximum amount of reactive power that can be injected by agent h . Usually $q_{min,h} < 0$ and $q_{max,h} > 0$.

In the following subsections, we propose three strategies where each agent can regulate the injection of reactive power into the grid in order to maintain the voltages magnitudes

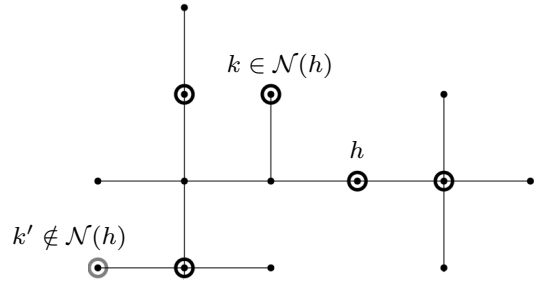


Figure 2. An example of neighbor agents in the cyber layer. Circled nodes (both gray and black) are agents (nodes in \mathcal{C}). Nodes circled in black belong to the set $\mathcal{N}(h) \subset \mathcal{C}$. Node circled in gray are agents which do not belong to the set of neighbors of h . For each agent $k \in \mathcal{N}(h)$, the path that connects h to k does not include any other agent besides h and k themselves.

within the interval $[U_{min}, U_{max}]$. The first two strategies are purely local, in the sense that

- 1) agent h updates the injection of q_h based only on measurements of its own voltage, i.e., u_h ;
- 2) agents do not communicate with each other.

Instead, in the third strategy agents are allowed to communicate (via some communication channels which could be possibly the power line communication (PLC)) exchanging information related to the taken measurements and to some additional quantities, as we will see in Subsection V. To model the admissible communications among the agents in the cyber layer, we next define the set of neighbors of a given agent h .

Definition 3 (Neighbors in the cyber layer): Let $h \in \mathcal{C}$ be an agent of the cyber layer. The set of neighbors of h in the cyber layer, denoted as $\mathcal{N}(h)$, is the subset of \mathcal{C} defined as

$$\mathcal{N}(h) = \{k \in \mathcal{C} \cup \{1\} \mid \exists \mathcal{P}_{hk}, \mathcal{P}_{hk} \cap \mathcal{C} = \{h, k\}\}.$$

In Figure 2 we report an example of the neighbors set. In our setup we assume that every agent $h \in \mathcal{C}$ knows its neighbors, i.e., $\mathcal{N}(h)$, and that it can communicate with them. In all strategies we assume that all agents measure synchronously their phasorial voltages at time-instants t_0, t_1, \dots , where $t_k = kT$, for a given sampling time T .

A. A first local voltage control strategy (denoted hereafter as LVC-1)

In this subsection, we propose a slightly modified version of the reactive power compensation technique which has been introduced in [4]. Let $f_h(u)$ be the function defined as

$$f_h(u) = m_h|u| + \beta_h \quad (12)$$

where

$$m_h = -\frac{q_h^M}{U_N - U_{min}}, \quad \beta_h = \frac{U_N q_h^M}{U_N - U_{min}}$$

Moreover let $\hat{f}_h(u)$ be the saturated version of $f_h(u)$ outside the interval $[q_{min,h}, q_{max,h}]$, that is,

$$\hat{f}_h(u) = [f_h(u)]_{q_{min,h}}^{q_{max,h}}.$$

In Figure 3, a pictorial description of both f_h and \hat{f}_h is provided. In the LVC-1, agent h , after having taken the measurement $u_h(t)$, updates $q_h(t)$ as follows

$$q_h(t+1) = [q_h(t) + \alpha_h(f_h(u_h(t)) - q_h(t))]_{q_{min,h}}^{q_{max,h}} \quad (13)$$

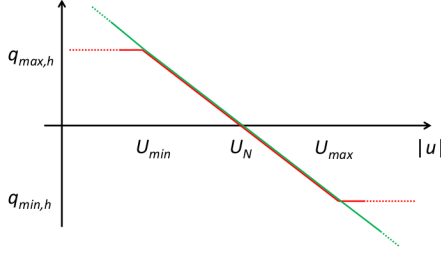


Figure 3. The green line represent function f_h , while the red line represents \hat{f}_h

where α_h is a positive constant. Observe that $\hat{f}_h(u)$ describes the equilibrium point for Equation (13); indeed, if $q_h(t) = \hat{f}_h(u_h(t))$ then $q_h(t+1) = q_h(t)$. In addition notice that $\hat{f}_h(U_N) = 0$. Roughly speaking, the rationale behind LVC-1 is the following: if $|u_h| < U_N$ then agent h will inject reactive power in order to increase $|u_h|$, while if $|u_h| > U_N$ then agent h will absorb reactive power in order to decrease $|u_h|$.

In next Proposition we characterize the convergence properties of (13), by adopting the approximation (9) for the voltage magnitudes, i.e. by neglecting the infinitesimal terms $o(1/U_N)$ in Equation (8).

Proposition 4: Consider algorithm (13), and let $\rho(M)$ be the spectral radius of the matrix M . Then, if

$$\alpha_h \leq \frac{2}{\frac{m_h}{\max\{m_j\}} - \frac{m_h \sin \theta \rho(M)}{U_N}}, \quad (14)$$

there exist a m -upla $(\bar{u}_1, \dots, \bar{u}_m)$ such that $u_h(t) \rightarrow \bar{u}_h$ and $q_h(t) \rightarrow \hat{f}_h(\bar{u}_h)$ for all $h \in \{1, \dots, m\}$.

Due to lack of space, the proofs of Proposition 4 and of the following Propositions are here omitted. Although LVC-1 is based on the quite popular voltage control strategy introduced in [4], it is not guaranteed that $|\bar{u}_h|$ lies within the interval $[U_{min}, U_{max}]$. In Section VI we will provide an example where the constraints (10) are violated at the steady state. However from the simulations we can see that the LVC-1 tends to approach the voltages outside the feasible region towards the interval defined in (10).

B. A second local voltage control strategy (denoted hereafter as LVC-2)

In this subsection we propose a local control strategy aiming at driving all the compensators' voltage magnitudes to a desired value u_d . The reactive power update is given by

$$q_h(t+1) = [q_h(t) + \epsilon(u_d - |u_h(t)|)]_{q_{min,h}^{max,h}} \quad (15)$$

The rationale behind the LVC-2 is based on the approximated linear relation among voltages and powers described in (9). Specifically, if $u_d - |u_h(t)| \geq 0$, then agent h will increase q_h , otherwise it will decrease it. The convergence of algorithm (15) is analyzed in the following Proposition. Again, the result stated has been obtained by adopting the approximation (9) for the voltage magnitudes.

Proposition 5: Consider algorithm (15). Then, if

$$\epsilon \leq \frac{2|u_0|}{\sin \theta \rho(M)} \quad (16)$$

there exist a m -upla $(\bar{u}_1, \dots, \bar{u}_m)$ such that $u_h(t) \rightarrow \bar{u}_h$ for all $h \in \{1, \dots, m\}$.

In general, the above Proposition does not guarantee that $u_h = u_d$ and, in turn, that $|u_h| \in [U_{min}, U_{max}]$ even if $u_d \in [U_{min}, U_{max}]$.

C. Distributed optimal reactive power flow algorithm (denoted hereafter as DORPF)

In this section we briefly review the algorithm proposed in [13], solving the following OPRF problem

$$\min_{q_G} \bar{u}^T Y u \cos \theta \quad (17a)$$

$$\text{subject to} \quad \begin{aligned} U_{min} &\leq |u_h| \leq U_{max} \\ q_{min,h} &\leq q_h \leq q_{max,h} \end{aligned} \quad \forall h \in \mathcal{C} \setminus \{0\} \quad (17b)$$

where $u^T Y u \cos \theta$ are the active power losses in the distribution lines. The algorithm solves problem (17) through a dual ascent strategy introducing the auxiliary variables λ_{min} , λ_{max} , μ_{min} , μ_{max} (the *Lagrange multipliers*, i.e. the dual variables of the problem). Agent h iteratively executes the following steps:

- 1) it measures its voltage $u_h(t)$ and it gathers from its neighbors the voltage measurements

$$\{u_k(t) = |u_k(t)|e^{i\angle u_k(t)}, k \in \mathcal{N}(h)\}$$

and the set of values of the Lagrange multipliers

$$\{\mu_{min,k}(t), \mu_{max,k}(t), k \in \mathcal{N}(h)\};$$

- 2) it updates the voltage Lagrange multipliers

$$\lambda_{min,h}(t+1) = \left[\lambda_{min,h}(t) + \frac{\gamma}{U_N^2} (U_{min}^2 - |u_h(t)|^2) \right]_0^\infty \quad (18a)$$

$$\lambda_{max,h}(t+1) = \left[\lambda_{max,h}(t) + \frac{\gamma}{U_N^2} (|u_h(t)|^2 - U_{max}^2) \right]_0^\infty \quad (18b)$$

where γ is a positive constant;

- 3) it computes the reactive power output

$$\begin{aligned} \bar{q}_h &= q_h(t) - \sin \theta (\lambda_{max,h}(t+1) - \lambda_{min,h}(t+1)) + \\ &+ \sum_{k \in \mathcal{N}(h)} G_{hk} |u_h(t)| |u_k(t)| \sin(\angle u_k(t) - \angle u_h(t) + \theta) \\ &- \sum_{k \in \mathcal{N}(h) \setminus \{0\}} G_{hk} (\mu_{max,k}(t) - \mu_{min,k}(t)). \end{aligned} \quad (19a)$$

where G_{hk} is the admittance of the electric path between h and k , which is assumed known by agent h .

- 4) it updates the power Lagrange multipliers

$$\mu_{min,h}(t+1) = \left[\mu_{min,h}(t) + \frac{\gamma}{U_N^2} (q_{min} - \bar{q}_h) \right]_0^\infty \quad (20a)$$

$$\mu_{max,h}(t+1) = \left[\mu_{max,h}(t) + \frac{\gamma}{U_N^2} (\bar{q}_h - q_{max}) \right]_0^\infty \quad (20b)$$

- 5) it projects the reactive power set point \bar{q}_h into the feasible set defined by equation (11) and injects it

$$q_h(t+1) = [\bar{q}_h]_{q_{min,h}^{max,h}} \quad (21)$$

The DORPF algorithm convergence properties are discussed in [13], where it is shown that under condition

$$\gamma \leq \frac{U_N^2}{\rho(\Phi M^{-1} \Phi^T)}, \quad (22)$$

where Φ is the matrix

$$\Phi = [-\sin \theta M \quad \sin \theta M \quad -I \quad I]^T,$$

the trajectory $t \rightarrow q(t)$ converges to the optimal solution of (17). In spite of the purely local algorithms LVC-1 and LVC-2, in DORPF the agents are allowed to communicate with each other. Thanks to the additional information gathered from the neighbors, the agents can not only drive the voltage magnitudes within the interval of admissible values, but also minimize the power losses.

Based on numerical evidence, the speed of convergence of DORPF to the steady-state of is slower than the speed of the two previous algorithms which, however, do not guarantee that the constraints (10) are satisfied. In next Section we introduce an algorithm that combines the fast transient of LVC-1 and LVC-2, with the asymptotic convergence to the optimal solution of (19) of DORPF.

V. FAST DISTRIBUTED OPTIMAL REACTIVE POWER FLOW ALGORITHM (DENOTED HEREAFTER F-DORPF)

In this section we propose a novel algorithm for voltage regulation and loss minimization, obtained by combining the strategies presented in the previous Section. In particular f-DORPF inherits the good properties of the former algorithms: the fast transient of algorithm LVC-1 and the convergence to an optimal equilibrium of algorithm DORPF. Finally, it exploits LVC-2 in order to avoid the use of the Lagrange multipliers associated with the voltage constraints (10). At every synchronous iteration t of the algorithm, each agent $h \in \mathcal{C} \setminus \{0\}$ executes the following operations in order:

- 1) it measures its voltage $u_h(t)$ and it gathers from its neighbors the phasorial voltage measurements

$$\{u_k(t), k \in \mathcal{N}(h)\}$$

and the values of the Lagrange multipliers associated to the reactive powers

$$\{\mu_{\max,k}(t), \mu_{\min,k}(t), k \in \mathcal{N}(h)\};$$

- 2) it determines the reactive power to be injected

$$\bar{q}_h = q_h(t) + \delta$$

where δ is computed as follows. If $|u_h(t)| \notin [U_{\min}, U_{\max}]$ then

$$\delta = \alpha_h(f_h(u_h(t)) - q_h(t)) \quad (23)$$

where α_h satisfies (14). Otherwise if $|u_h(t)| \in [U_{\min}, U_{\max}]$, then agent h computes the quantities

$$\delta_D = \sum_{k \in \mathcal{N}(h)} G_{hk}(|u_h(t)||u_k(t)| \sin(\angle u_k(t) - \angle u_h(t) - \theta) - \mu_{\max,k}(t) + \mu_{\min,k}(t)) \quad (24)$$

$$\delta_{U_{\max}} = \epsilon((U_{\max} - |u_h(t)|)) \quad (25)$$

$$\delta_{U_{\min}} = \epsilon((U_{\min} - |u_h(t)|)) \quad (26)$$

where ϵ satisfies (16). Since the constraints (10) are satisfied, $\delta_{U_{\max}}$ and $\delta_{U_{\min}}$ have opposite signs, i.e. they would update the reactive power injected in opposite directions. Let δ be the value between $\delta_{U_{\max}}$ and $\delta_{U_{\min}}$ with the same sign of δ_D . Agent h will set

$$\delta = \text{sign}(\delta_D) \min\{|\delta|, |\delta_D|\}$$

- 3) it computes the reactive power to be injected

$$\bar{q}_h = q_h(t) + \delta$$

- 4) it updates the power multipliers as

$$\mu_{\min,h}(t+1) = \left[\mu_{\min,h}(t) + \gamma \left(\frac{q_{\min,h}}{U_N^2} - \frac{\bar{q}_h}{U_N^2} \right) \right]_0^\infty \quad (27)$$

$$\mu_{\max,h}(t+1) = \left[\mu_{\max,h}(t) + \gamma \left(\frac{\bar{q}_h}{U_N^2} - \frac{q_{\max,h}}{U_N^2} \right) \right]_0^\infty \quad (28)$$

- 5) it injects the projected set point

$$q_h(t+1) = [\bar{q}_h(t)]_{q_{\min,h}^{q_{\max,h}}} \quad (29)$$

Loosely speaking, the f-DORPF works as follows: if $|u_h|$ violates the constraints (10), node h updates the reactive power injection performing a step of the LVC-1, because it provides a faster response approaching the system towards a feasible configuration. Otherwise, in order to keep the constraints satisfied, it discriminates between a step inspired by the DORPF (except for the voltages multipliers), and a step which is suggested by LVC-2 (the choice is for the less aggressive update).

VI. SIMULATIONS AND DISCUSSION

The algorithms has been simulated on the testbed IEEE 37 [15], sketched in Figure 4, which is a portion of 4.8kV power distribution network located in California. The load buses are a mix of constant-current, constant-impedance and constant-power loads, with a total active power demand of almost 2 MW and reactive power demand of almost 1 MVAR (see [15] for the testbed data). The impedance of the power lines differs from edge to edge, however, the inductance/resistance ratio exhibits a smaller variation, ranging from $\angle z_e = 0.47$ to $\angle z_e = 0.59$, thus justifying Assumption 1. We consider the scenario in which five micro-generators, the gray nodes in Figure 4, can inject or absorb reactive power to regulate the voltage magnitude.

In all the following simulations, the initial micro-generators reactive power outputs are set to zero, and their generation capabilities are such that there exists always a configuration guaranteeing that the constraints (10) are satisfied. In Figure 5 and in Figure 6 we plot the behavior of, respectively, the minimum agents voltage magnitude and the power losses for the LVC-1, LVC-2 and DORPF strategies. The simulations have been obtained optimizing over the parameters α_h, ϵ and γ . The following observations are in turn:

- LVC-1 strategy fails to satisfy the voltage constraints;
- LVC-2 satisfies the voltage constraints but it attains a value of power losses which is very high as compared to the power losses of the other strategies;
- DORPF leads the voltage magnitudes within the set $[U_{\min}, U_{\max}]$ ¹ and the power losses to the optimal value (computed with a centralized solver) compatible with the voltage and power constraints; however it exhibits a transient which is much slower than the transients of the other two strategies.

In Figure 7 and in Figure 8 we compare the performance of the DORPF and f-DORPF algorithms. We can see that the

¹For simplicity in this simulation we consider only the constraint $|u_h| \geq U_{\min}$; however both LVC-2 and DORPF fulfill also the constraint $|u_h| \leq U_{\max}$.

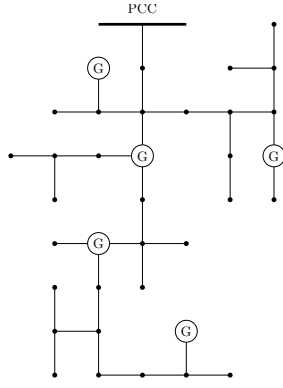


Figure 4. Schematic representation of the IEEE 37 test feeder [15], the grey nodes represent the agents in the distribution network.

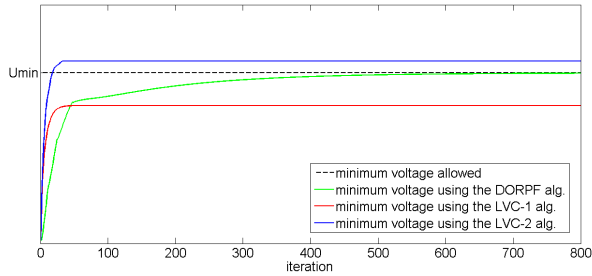


Figure 5. Minimum compensators voltage magnitude using the algorithms revised in Section IV.

f-DORPF strategy achieves the same optimal performance, in terms of power losses of the DORPF algorithm, but its convergence rate is much faster (comparable with the convergence rate of the LPV-1 algorithm). The little gap between the optimal power losses and the steady-state power losses attained by both f-DORPF and DORPF is due to the fact that these algorithms use a unique value of θ for all the lines, and that they approximate the voltages as linear function of the powers with (8) and (9).

REFERENCES

- [1] A. Ipakchi and F. Albuyeh, "Grid of the future," *Power and Energy Magazine, IEEE*, vol. 7, no. 2, pp. 52–62, 2009.
- [2] F. Katiraei and M. Iravani, "Power management strategies for a microgrid with multiple distributed generation units," *Power Systems, IEEE Transactions on*, vol. 21, no. 4, pp. 1821–1831, 2006.
- [3] M. E. Baran and F. F. Wu, "Optimal sizing of capacitors placed on a radial distribution system," *IEEE Trans. Power Del.*, vol. 4, no. 1, pp. 735–743, Jan. 1989.

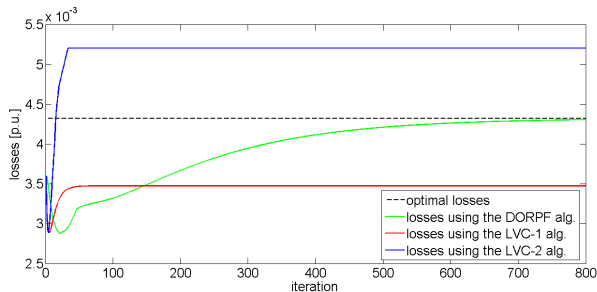


Figure 6. System losses using the algorithms revised in Section IV.

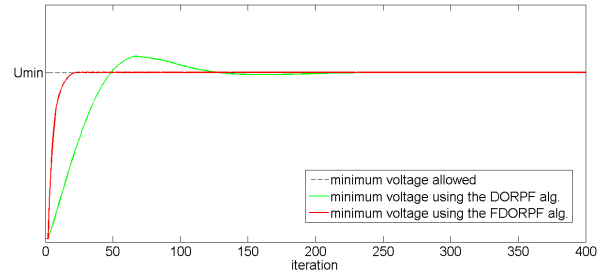


Figure 7. Comparison of the minimum compensators voltage magnitude trajectory using the DORPF and the FDORPF algorithms.

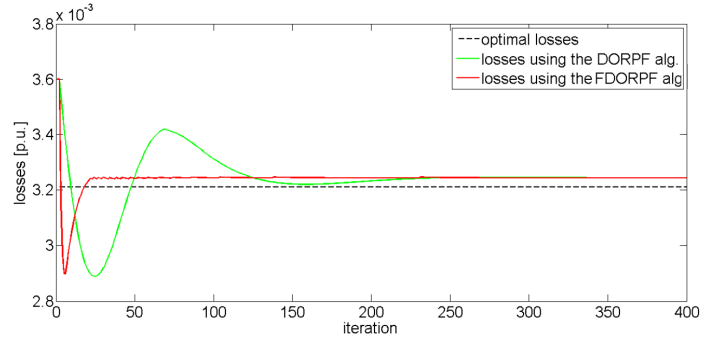


Figure 8. Comparison of the losses using the DORPF and the FDORPF algorithms.

- [4] K. Turitsyn, P. Šulc, S. Backhaus, and M. Chertkov, "Options for control of reactive power by distributed photovoltaic generators," *Proc. IEEE*, vol. 99, no. 6, pp. 1063–1073, Jun. 2011.
- [5] M. Juamperez, Y. Guangya, and S. B. Kjær, "Voltage regulation in lv grids by coordinated volt-var control strategies," *Journal of Modern Power Systems and Clean Energy*, vol. 2, no. 4, pp. 319–328, 2014.
- [6] J. Smith, W. Sunderman, R. Dugan, and B. Seal, "Smart inverter volt/var control functions for high penetration of pv on distribution systems," in *Power Systems Conference and Exposition (PSCE), 2011 IEEE/PES. IEEE*, 2011, pp. 1–6.
- [7] S. Kundu, S. Backhaus, and I. A. Hiskens, "Distributed control of reactive power from photovoltaic inverters," in *Circuits and Systems (ISCAS), 2013 IEEE International Symposium on*. IEEE, 2013, pp. 249–252.
- [8] N. Li, G. Qu, and M. Dahleh, "Real-time decentralized voltage control in distribution networks," in *Communication, Control, and Computing (Allerton), 2014 52nd Annual Allerton Conference on*. IEEE, 2014, pp. 582–588.
- [9] E. Dell'Anese, H. Zhu, and G. Giannakis, "Distributed optimal power flow for smart microgrids," *submitted to IEEE Transactions of Smart Grid*, 2013, arXiv preprint available [math.OC] 1211.5856.
- [10] J. Lavaei and S. H. Low, "Zero duality gap in optimal power flow problem," *IEEE Trans. Power Syst.*, 2011.
- [11] B. Zhang, A. Lam, A. Dominguez-Garcia, and D. Tse, "An optimal and distributed method for voltage regulation in power distribution systems," *Power Systems, IEEE Transactions on*, vol. PP, no. 99, pp. 1–13, 2014.
- [12] S. Bolognani, R. Carli, G. Cavraro, and S. Zampieri, "A distributed control strategy for optimal reactive power flow with power constraints," in *Decision and Control (CDC), 2013 IEEE 52nd Annual Conference on*. IEEE, 2013, pp. 4644–4649.
- [13] —, "Distributed reactive power feedback control for voltage regulation and loss minimization," *Automatic Control, IEEE Transactions on*, vol. 60, no. 4, pp. 966–981, April 2015.
- [14] A. G. Phadke and J. S. Thorp, *Synchronized phasor measurements and their applications*. Springer, 2008.
- [15] W. H. Kersting, "Radial distribution test feeders," in *IEEE Power Engineering Society Winter Meeting*, vol. 2, Jan. 2001, pp. 908–912.